# Supplementary material

## Experimental and theoretical evidences of the effect of the electronic structure and flexibility of the counteranion on the magnetization relaxation in $[Dy(L)_2(H_2O)_5]^{3+}$ (L = phosphine oxide derivative) pentagonal bipyramidal SIMs

Ismael F. Díaz-Ortega, Juan Manuel Herrera, Sourav Dey, Hiroyuki Nojiri, Gopalan Rajaraman, Enrique Colacio.

**Table S1**.- Continuous Shape Measures for **1**.

```
-----------------------------------------------------------------
S H A P E   v2.1. Continuous Shape Measures calculation (c) 2013
Electronic Structure Group, Universitat de Barcelona Contact:
llunell@ub.edu
-----------------------------------------------------------------

JETPY-7          7 C3v   Johnson elongated triangular pyramid J7
JPBPY-7          6 D5h   Johnson pentagonal bipyramid J13
CTPR-7           5 C2v   Capped trigonal prism
COC-7            4 C3v   Capped octahedron
PBPY-7           3 D5h   Pentagonal bipyramid
HPY-7            2 C6v   Hexagonal pyramid
HP-7             1 D7h   Heptagon

Structure [ML7 ]       JETPY-7      JPBPY-7       CTPR-7
COC-7       PBPY-7         HPY-7         HP-7
 Dy              ,      22.915,       3.085,       3.874,
5.235,       0.639,      24.338,      34.250
```

**Table S2**. Computed energy spectrum ($cm^{-1}$), g tensors, tilting angle (θ) of the main anisotropy axes of the first excited (ES1) KD with respect to the ground state (GS) KD for **1**.

| Energy ($cm^{-1}$) | $g_x$ | $g_y$ | $g_z$ | Angle between the anisotropy axis |
|---|---|---|---|---|
| 0.0 | 0.000 | 0.000 | 19.974 | |
| 341.7 | 0.017 | 0.024 | 17.086 | 3.7 |
| 508.5 | 0.716 | 1.774 | 17.815 | 84.5 |
| 554.4 | 2.971 | 3.367 | 10.589 | 18.4 |
| 582.8 | 0.200 | 5.262 | 10.900 | 72.8 |
| 630.1 | 0.595 | 3.662 | 7.204 | 155.9 |
| 682.7 | 1.391 | 2.587 | 12.555 | 43.6 |
| 778.1 | 0.090 | 0.229 | 18.410 | 121.1 |

**Table S3**. Computed energy spectrum ($cm^{-1}$), g tensors, angle (θ) between the anisotropy axis of the excited KD with respect to the ground state KD for **1a**.

| Energy ($cm^{-1}$) | $g_x$ | $g_y$ | $g_z$ | θ (°) |
|---|---|---|---|---|
| 0.0 | 0.000 | 0.000 | 19.979 | |
| 322.5 | 0.032 | 0.057 | 17.048 | 0.585 |
| 409.4 | 0.086 | 0.218 | 19.533 | 92.244 |
| 518.8 | 9.079 | 8.039 | 4.067 | |
| 552.3 | 3.424 | 4.160 | 8.348 | |
| 617.3 | 3.144 | 5.158 | 12.318 | |

| | | | | |
|---|---|---|---|---|
| 689.1 | 0.711 | 1.058 | 18.278 | |
| 741.1 | 0.004 | 0.126 | 19.313 | |

**Table S4**. Computed energy spectrum ($cm^{-1}$), g tensors, tilting angle (θ) of the main anisotropy axes of the first excited (ES1) KD with respect to the ground state (GS) KD for **1'a**.

| Energy ($cm^{-1}$) | $g_x$ | $g_y$ | $g_z$ | θ (°) |
|---|---|---|---|---|
| 0.0 | 0.000 | 0.000 | 19.978 | |
| 318.7 | 0.036 | 0.055 | 17.062 | 1.446 |
| 460.5 | 0.016 | 0.232 | 18.994 | 88.926 |
| 534.0 | 0.428 | 1.214 | 12.540 | |
| 562.7 | 10.908 | 7.012 | 2.309 | |
| 614.5 | 1.132 | 2.951 | 10.234 | |
| 650.7 | 0.709 | 1.199 | 16.548 | |
| 697.4 | 0.008 | 0.687 | 17.933 | |

**Table S5**. Relevant structural data for $[Dy(L)_2(H_2O)_5]^{3+}$ complexes.

| **$[Dy(L)_2(H_2O)_5]^{3+}$ SIMs** | O-Dy-O axial (°) | Average Dy-$O_{axial}$ (Å) | Average Dy-$O_w$ (Å) | Average $O_w$-Dy-$O_w$ (°) | Δ | Ref. |
|---|---|---|---|---|---|---|
| $[Dy(OPCy_3)(H_2O)_5](triflate)_3$ $\cdot 2OPCy_3$ (**1**) | 173.42 | 2.202 | 2.364 | 72.36 | 0.162 | T. w. |
| $[Dy(OPCy_3)(H_2O)_5]Br_3$ $\cdot 2OPCy_3 \cdot 2H_2O \cdot 2EtOH$ (**1a**) | 179.04 | 2.200 | 2.352 | 72.07 | 0.152 | 12a |
| $[Dy(OPCy_3)(H_2O)_5]Cl_3$ $\cdot OPCy_3 \cdot H_2O \cdot EtOH$ (**1'a**) | 175.79 | 2.220 | 2.359 | 72.03 | 0.139 | 12a |
| $[Dy(OP^tBu(NH^iPr)_2(H_2O)_5]I_3 \cdot$ $2OP^tBu(NH^iPr)_2 \cdot (H_2O)$ (**1b**) | 175.14 | 2.205 | 2.363 | 72.05 | 0.158 | 12d |
| $[Dy(HMPA)_2(H_2O)_5]I_3 \cdot 2HMPA$ (**1c**) | 177.97 | 2.205 | 2.359 | 72.02 | 0.154 | 12g |
| $[Dy(HMPA)_2(H_2O)_5]Cl_3 \cdot HMPA$ (**1c'**) | 176.14 | 2.219 | 2.348 | 72.04 | 0.129 | 12g |
| $[Dy(OPCyPh_2)(H_2O)_5]Br_3$ $\cdot 2OPCy_3 \cdot 3H_2O \cdot 2EtOH$ (**1d**) | 173.77 | 2.217 | 2.343 | 72.04 | 0.126 | 12f |

**Table S6**. LoProp charges for **1.**

| Atom | LoProp charge |
|---|---|
| Dy | 2.5818 |
| O4 | -0.7311 |
| O7 | -0.7413 |
| O10 | -1.1297 |
| O11 | -1.1254 |
| O12 | -0.7450 |
| O15 | -0.7370 |
| O20 | -0.7426 |

**Table S7.** LoProp charges for **1a**

| Atom | LoProp charge |
|---|---|
| Dy | 2.6082 |
| O4 | -0.1164 |
| O7 | -0.1127 |
| O6 | -0.7646 |
| O9 | -0.7595 |
| O12 | -0.7625 |
| O15 | -0.7570 |
| O18 | -0.7656 |

**Table S8.** LoProp charges for **1'a**.

| Atom | LoProp charge |
|---|---|
| Dy | 2.6089 |
| O4 | -1.1260 |
| O5 | -0.1152 |
| O6 | -0.7368 |
| O9 | -0.7732 |
| O12 | -0.7669 |
| O15 | -0.7669 |
| O18 | -0.7560 |

**Table S9**. LoProp charges for **1A.**

| Atom | LoProp Charge |
|---|---|
| Dy | 2.5821 |
| O1(axial) | -1.1487 |
| O2(axial) | -1.1439 |
| O3(equatorial) | -0.6883 |
| O4(equatorial) | -0.6857 |
| O5(equatorial) | -0.7421 |
| O6(equatorial) | -0.7269 |

| | |
|---|---|
| O7(equatorial) | -0.6854 |

**Table S10**. LoProp charges for **1B.**

| **Atom** | **LoProp Charge** |
|---|---|
| Dy | 2.5842 |
| O1(axial) | -1.1732 |
| O2(axial) | -1.1684 |
| O3(equatorial) | -0.6802 |
| O4(equatorial) | -0.6895 |
| O5(equatorial) | -0.6809 |
| O6(equatorial) | -0.6943 |
| O7(equatorial) | -0.6722 |

**Table S11**. LoProp charges for **1C.**

| **Atom** | **LoProp Charge** |
|---|---|
| Dy | 2.5842 |
| O1(axial) | -1.2080 |
| O2(axial) | -1.2112 |

**Table S12**. Computed energy spectrum ($cm^{-1}$), g tensors, angle (θ) between the anisotropy axis of the excited KD with respect to the ground state KD for **1A**.

| Energy ($cm^{-1}$) | $g_x$ | $g_y$ | $g_z$ | θ (°) |
|---|---|---|---|---|
| 0.0 | 0.000 | 0.000 | 19.97 | |
| 395.0 | 0.007 | 0.009 | 17.071 | 2.711 |
| 660.7 | 0.968 | 2.516 | 13.413 | 25.598 |
| 697.7 | 0.631 | 2.629 | 14.905 | 75.709 |
| 782.9 | 2.109 | 5.708 | 11.448 | 71.556 |
| 840.9 | 2.670 | 4.461 | 12.021 | 101.422 |
| 893.7 | 0.641 | 1.354 | 16.759 | 64.576 |
| 946.3 | 0.188 | 0.980 | 18.013 | 117.153 |

**Table S13**. Computed energy spectrum ($cm^{-1}$), g tensors, angle (θ) between the anisotropy axis of the excited KD with respect to the ground state KD for **1B**.

| Energy ($cm^{-1}$) | $g_x$ | $g_y$ | $g_z$ | θ (°) |
|---|---|---|---|---|
| 0.0 | 0.000 | 0.000 | 19.981 | |
| 463.8 | 0.004 | 0.004 | 17.050 | 1.918 |
| 811.5 | 0.024 | 0.031 | 14.305 | 7.318 |
| 997.3 | 2.704 | 4.262 | 13.243 | 63.449 |
| 1032.6 | 8.371 | 6.579 | 1.399 | 29.978 |
| 1085.3 | 2.971 | 4.367 | 9.620 | 91.553 |
| 1120.4 | 1.455 | 2.091 | 11.789 | 59.530 |

| | | | | |
|---|---|---|---|---|
| 1181.5 | 0.261 | 1.203 | 17.380 | 115.638 |

**Table S14**. Computed energy spectrum ($cm^{-1}$), g tensors, angle (θ) between the anisotropy axis of the excited KD with respect to the ground state KD for **1C**.

| Energy ($cm^{-1}$) | $g_x$ | $g_y$ | $g_z$ | θ (°) |
|---|---|---|---|---|
| 0.0 | 0.000 | 0.000 | 20.013 | |
| 642.6 | 0.000 | 0.000 | 16.963 | 0.191 |
| 1249.0 | 0.000 | 0.000 | 14.050 | 0.213 |
| 1746.2 | 0.001 | 0.001 | 11.388 | 0.568 |
| 2065.6 | 0.236 | 0.238 | 8.957 | 3.029 |
| 2209.8 | 0.013 | 0.449 | 6.723 | 165.091 |
| 2249.3 | 7.919 | 6.626 | 2.098 | 18.186 |
| 2256.8 | 0.887 | 4.028 | 15.170 | 83.592 |

**Table S15.** Crystallographic data for complex **1.**

| | |
|---|---|
| Empirical formula | $C_{75}H_{141.37}DyF_9O_{18}P_4S_3$ |
| Formula weight | 1884.80 |
| Temperature/K | 100.0 |
| Crystal system | monoclinic |
| Space group | $P2_1$ |
| a/Å | 15.6605(8) |
| b/Å | 18.6140(8) |
| c/Å | 15.9083(8) |
| β/° | 104.6559(17) |
| Volume/$Å^3$ | 4486.5(4) |
| Z | 2 |
| $\rho_{calc}g/cm^3$ | 1.395 |
| $\mu/mm^{-1}$ | 1.054 |
| F(000) | 1981.0 |
| Crystal size/$mm^3$ | 0.15 × 0.13 × 0.12 |
| Radiation | MoKα (λ = 0.71073) |
| 2Θ range for data collection/° | 4.756 to 49.62 |
| Index ranges | $-18 \leq h \leq 18$, $-21 \leq k \leq 21$, $-18 \leq l \leq 18$ |
| Reflections collected | 85027 |
| Independent reflections | 15379 [$R_{int}$ = 0.0355, $R_{sigma}$ = 0.0227] |
| Data/restraints/parameters | 15379/125/1098 |
| Goodness-of-fit on $F^2$ | 1.112 |
| Final R indexes [I>=2σ (I)] | $R_1$ = 0.0214, $wR_2$ = 0.0525 |
| Final R indexes [all data] | $R_1$ = 0.0225, $wR_2$ = 0.0534 |
| Largest diff. peak/hole / e $Å^{-3}$ | 0.39/-0.69 |
| Flack parameter | -0.032(3) |

**Table S16.-** Selected bond distances (Å) for complex **1**.

| | |
|---|---|
| Dy1-O1 | 2.200(2) |
| Dy1-O2 | 2.203(2) |
| Dy1-O1W | 2.355(3) |
| Dy1-O2W | 2.368(2) |
| Dy1-O3W | 2.354(3) |
| Dy1-O4W | 2.369(2) |
| Dy1-O5W | 2.363(2) |

**Table S17.-** Selected bond angles (º) for complex **1**.

| | |
|---|---|
| O1-Dy1-O2 | 173.42(10) |
| O1-Dy1-O1W | 87.22(10) |
| O1-Dy1-O2W | 88.33(10) |
| O1-Dy1-O3W | 99.14(10) |
| O1-Dy1-O4W | 87.18(11) |
| O1-Dy1-O5W | 94.30(9) |
| O2-Dy1-O1W | 86.20(10) |
| O2-Dy1-O2W | 90.10(10) |
| O2-Dy1-O3W | 86.46(10) |
| O2-Dy1-O4W | 97.94(11) |
| O2-Dy1-O5W | 83.46(9) |
| O1W-Dy1-O2W | 74.06(8) |
| O1W-Dy1-O3W | 145.50(9) |
| O1W-Dy1-O4W | 142.92(8) |
| O1W-Dy1-O5W | 72.27(9) |
| O2W-Dy1-O3W | 72.29(9) |
| O2W-Dy1-O4W | 142.29(8) |
| O2W-Dy1-O5W | 146.05(8) |
| O3W-Dy1-O4W | 71.54(9) |
| O3W-Dy1-O5W | 139.94(9) |
| O4W-Dy1-O5W | 71.65(8) |

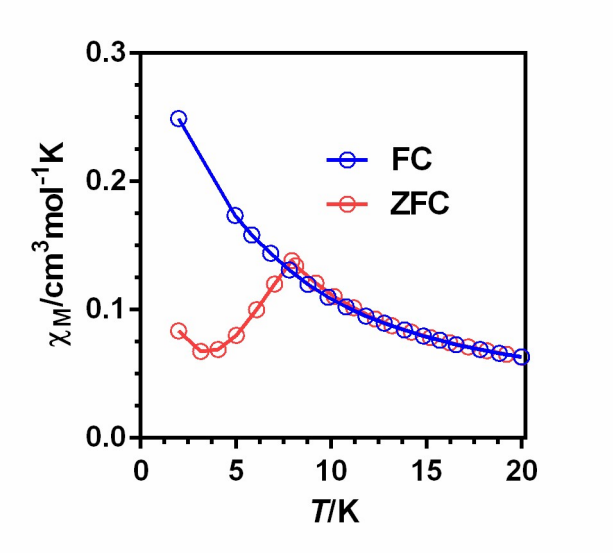


**Figure S1**.- Temperature dependence of zero-field cooled (red) and field cooled (blue) magnetization for **1@Y**.

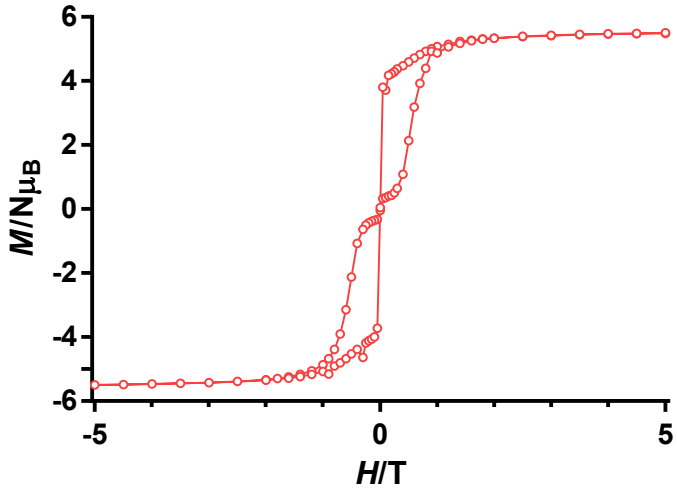


**Figure S2**.- Hysteresis plot for compound **1** at 2 K and field sweep rate of 1.8 mT s$^{-1}$.

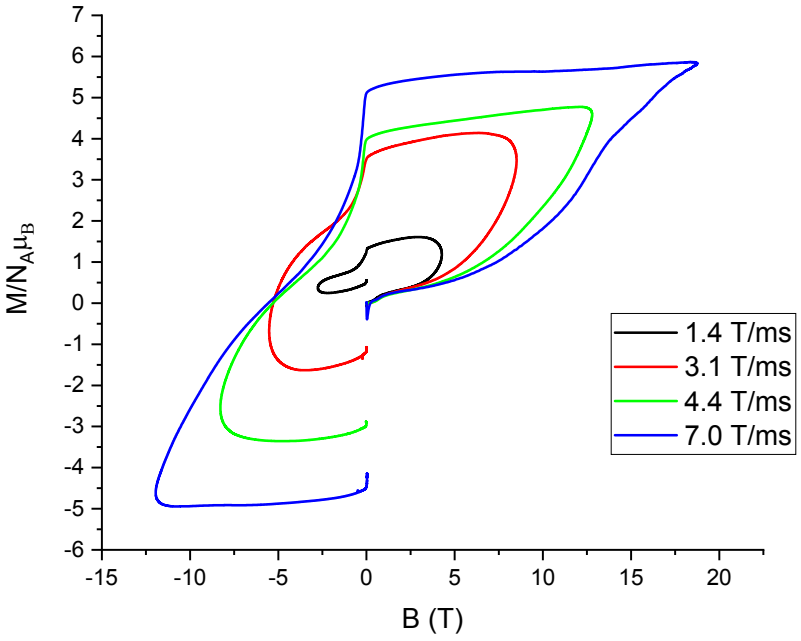


**Figure S3**. Pulsed-field magnetization curves for **1** at 1.6 K and at the indicated field sweep rates.

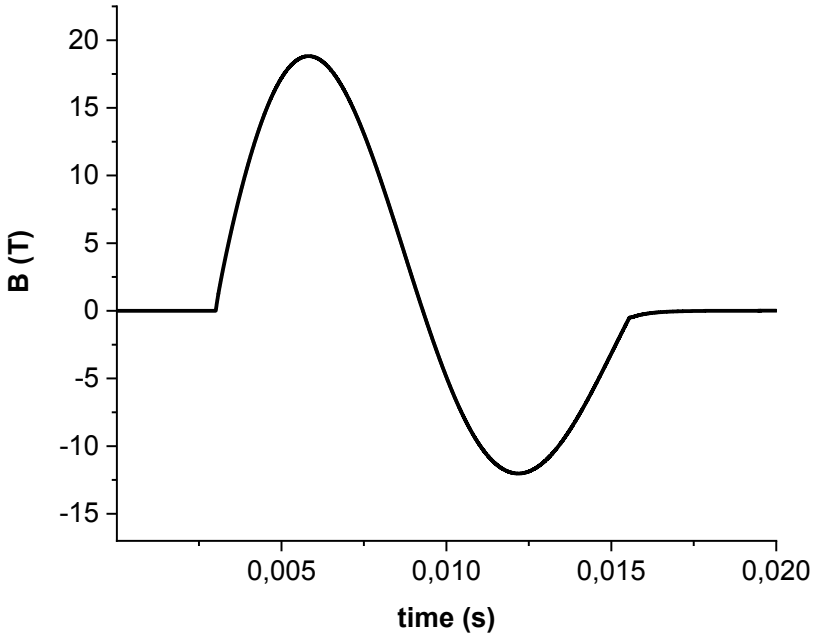


**Figure S4**. Field-scan sequence as a function of time for a maximum field of 18.7 T.

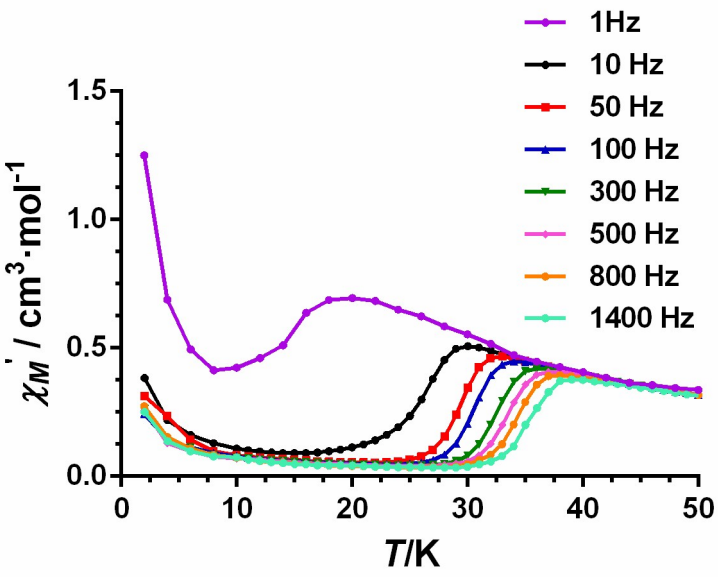


**Figure S5**. Temperature dependence of the nn-phase ac magnetic susceptibility ($\chi'_M$) for compound **1**.

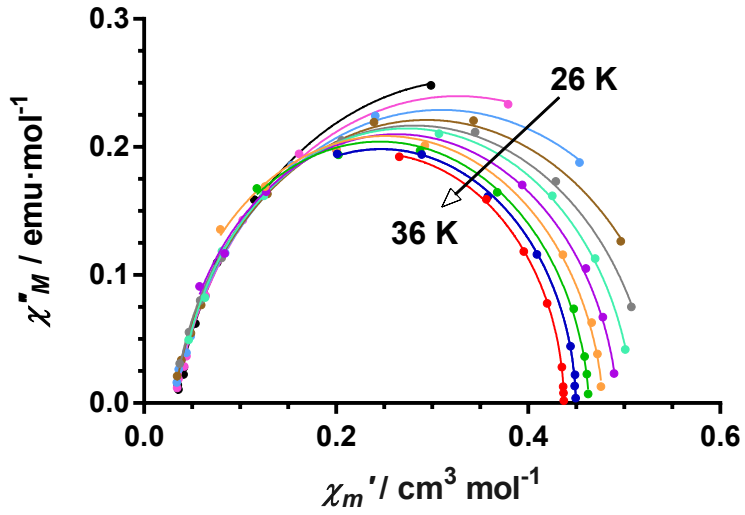


**Figure S6**. Cole-Cole plot for compound **1**.

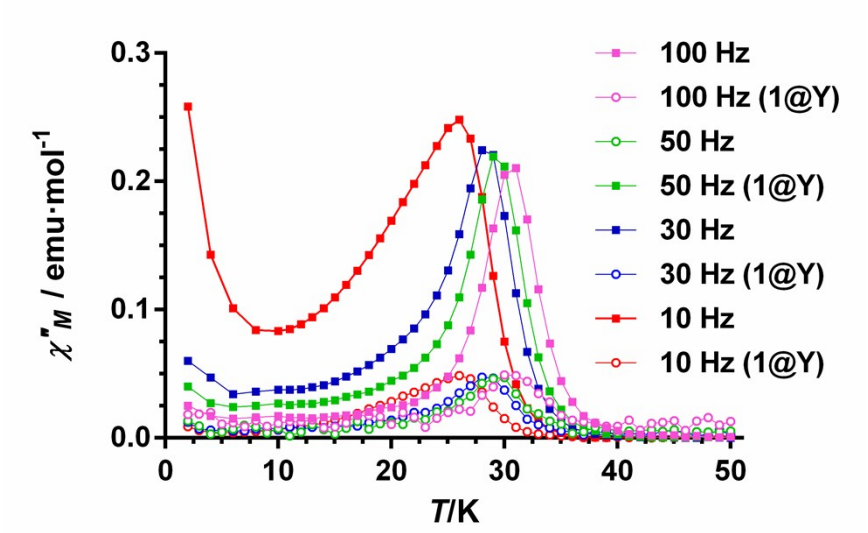


**Figure S7**. Comparison of the temperature dependence of the $\chi''_M$ signals for **1** and **1@Y**.

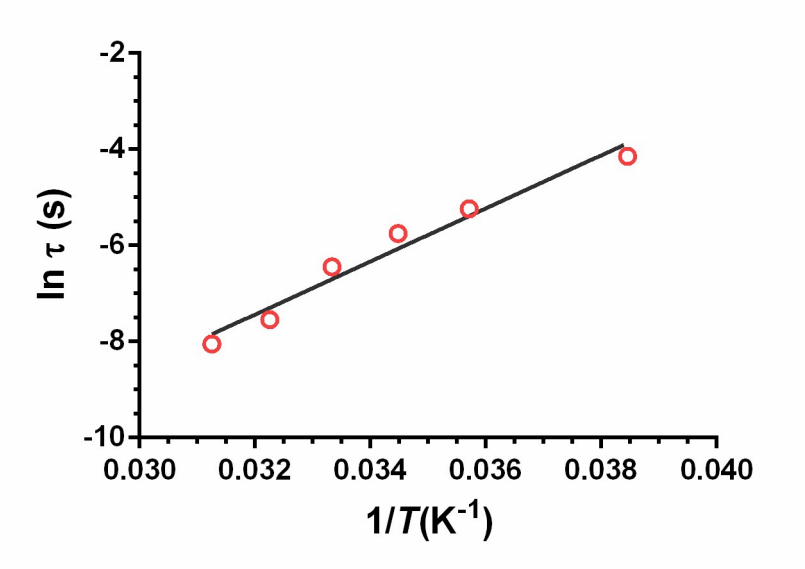


**Figure S8**. Arrhenius plot for **1@Y**.

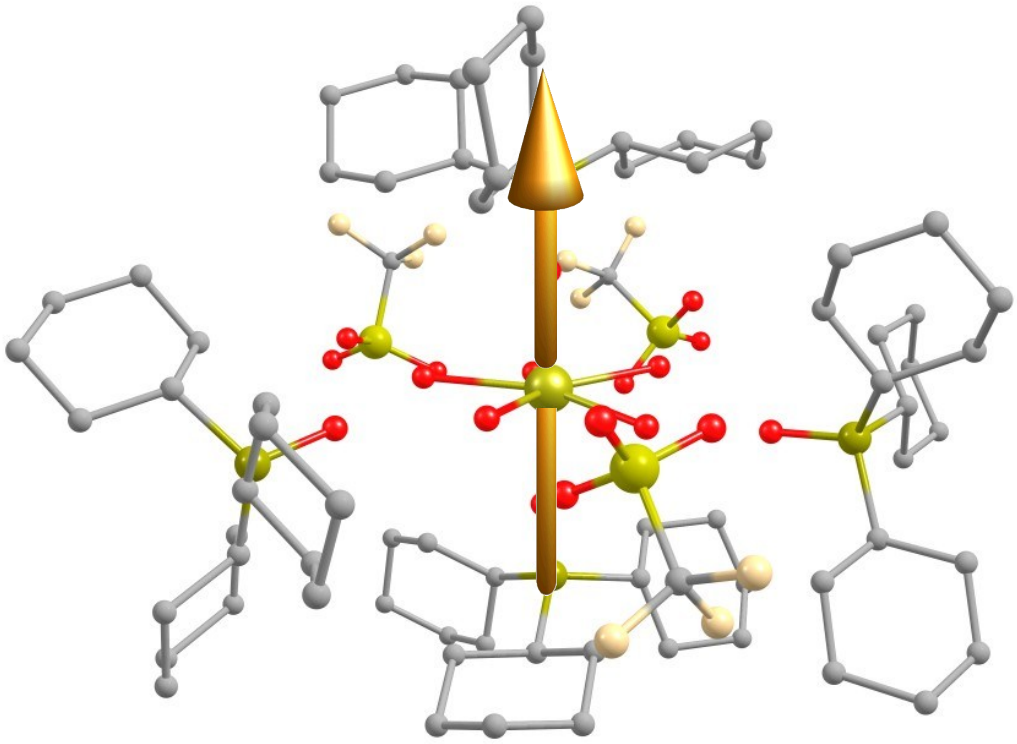

**Figure S9:** The anisotropy axis of complex **1**. Colour code: Dy: light yellow, S: greenish yellow, P: yellow, F: light pink, C: grey. Hydrogens are omitted for clarity.

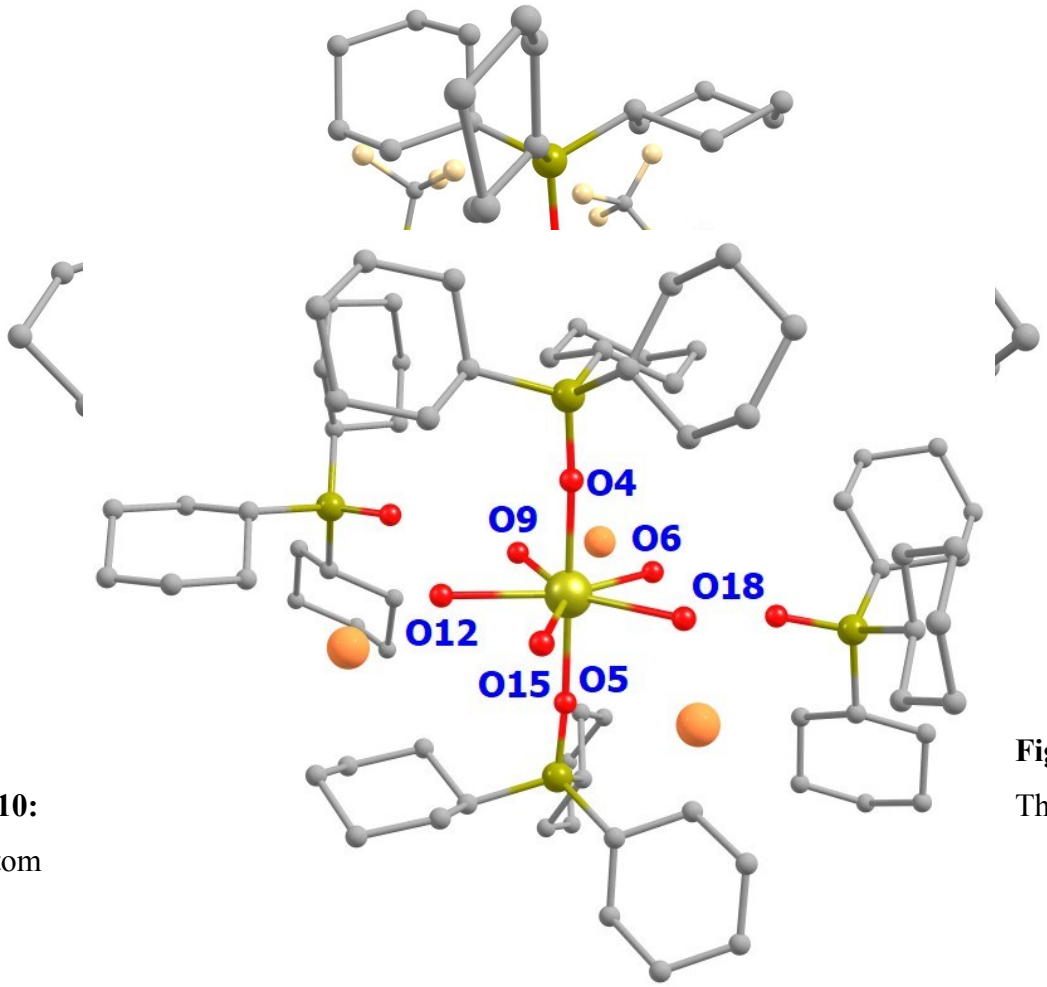


**Figure S10:** The atom numbering scheme for the LoProp charge of complex **1**. Colour code: Dy: light yellow, S: greenish yellow, P: yellow, F: light pink, O: red C: grey. Hydrogens are omitted for clarity.

**Figure S11:** The atom numbering scheme for the LoProp charge of complex **1a**. Colour code: Dy: light yellow, P: yellow, Br: brown, O: red C: grey. Hydrogens are omitted for clarity.

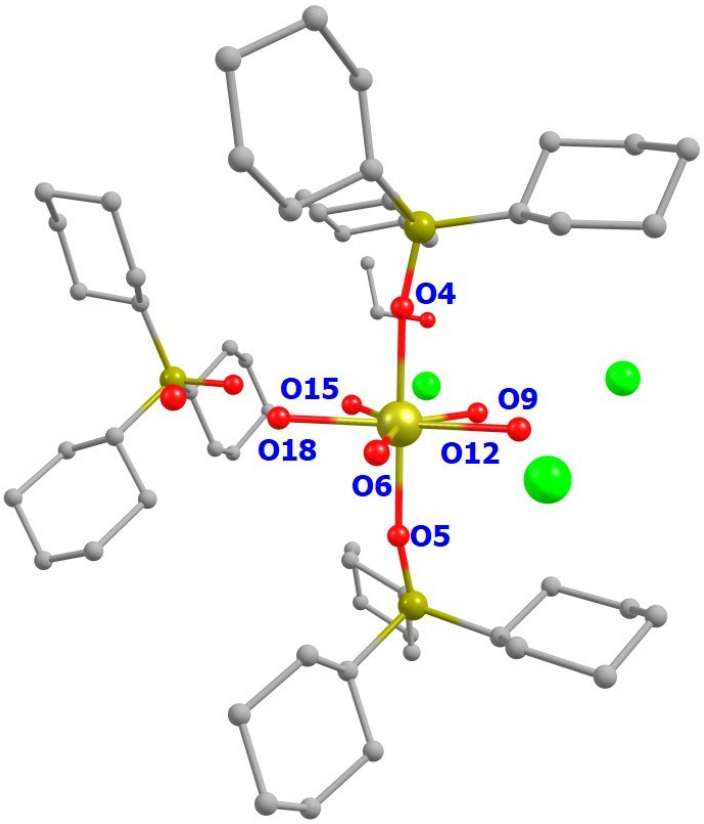


**Figure S12:** The atom numbering scheme for the LoProp charge of complex **1'a**. Colour code: Dy: light yellow, P: yellow, Cl: green, O: red C: grey. Hydrogens are omitted for clarity.

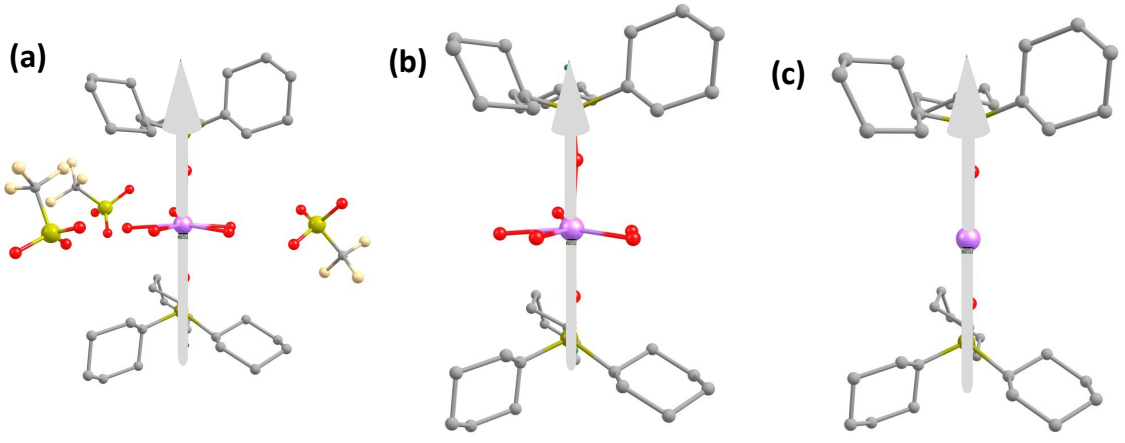

**Figure S13:** The anisotropy axis of (a) **1A** (b) **1B** (c) **1C**. Colour code: Dy: blue violet, P: yellow, Cl: green, O: red C: grey. Hydrogens are omitted for clarity.

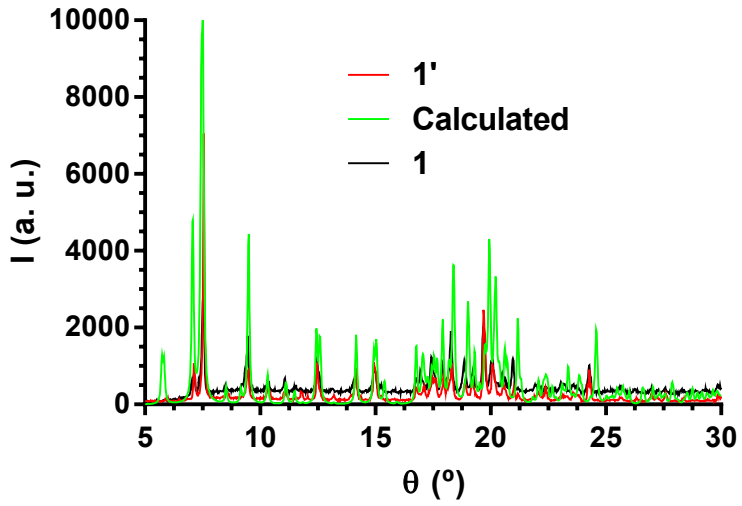


**Figure S14**: X-ray powder diffractograms for **1** (black), **1'** (red) and the calculated from the X-ray crystal structure (green).